Alternative Versions of the Myosin Relay Domain Differentially Respond to Load to Influence *Drosophila* Muscle Kinetics

Chaoxing Yang,*† Seemanti Ramanath,*† William A. Kronert,‡§ Sanford I. Bernstein,‡§ David W. Maughan,¶ and Douglas M. Swank*†

*Department of Biology and †Center for Biotechnology and Interdisciplinary Studies, Rensselaer Polytechnic Institute, Troy, New York; ‡Biology Department and §Molecular Biology Institute, San Diego State University, San Diego, California; and ¶Department of Molecular Physiology and Biophysics, University of Vermont, Burlington, Vermont

ABSTRACT We measured the influence of alternative versions of the *Drosophila melanogaster* myosin heavy chain relay domain on muscle mechanical properties. We exchanged relay domain regions (encoded by alternative versions of exon 9) between an embryonic (EMB) isoform and the indirect flight muscle isoform (IFI) of myosin. Previously, we observed no effect of exchanging the EMB relay domain region into the flight muscle isoform (IFI-9b) on in vitro actin motility velocity or solution ATPase measurements compared to IFI. However, in indirect flight muscle fibers, IFI-9b exhibited decreased maximum power generation (P_{max}) and optimal frequency of power generation (f_{max}) to 70% and 83% of IFI fiber values. The decrease in muscle performance reduced the flight ability and wing-beat frequency of IFI-9b *Drosophila* compared to IFI *Drosophila*. Previously, we found that exchanging the flight muscle specific relay domain into the EMB isoform (EMB-9a) prevented actin movement in the in vitro motility assay compared to EMB, which does support actin movement. However, in indirect flight muscle fibers EMB-9a was a highly effective motor, increasing P_{max} and f_{max} 2.5-fold and 1.4-fold, respectively, compared to fibers expressing EMB. We propose that the oscillatory load EMB-9a experiences in the muscle fiber reduces a high activation energy barrier between two strongly bound states of the cross-bridge cycle, thereby promoting cross-bridge cycling. The IFI relay domain's enhanced sensitivity to load increases cross-bridge kinetics, whereas the EMB version is less load-sensitive.

INTRODUCTION

The expression of specific myosin isoforms, a major source of functional diversity in striated muscle, enables specialized muscle fiber types to respond to different locomotory demands. Myosin isoforms are the primary determinants of shortening velocity or optimal muscle operational frequency, force, and power-generating ability (1). Sequence comparisons and in vitro functional studies at the molecular level suggest that specific structural domains of the myosin heavy chain (MHC) modulate myosin functional properties (2–5). However, the importance of these domains in setting muscle mechanical properties has only been directly tested in organized muscle of mammalian smooth muscle, *Drosophila* muscle, and mouse cardiac muscle (6–10).

Utilizing the highly developed genetics of *Drosophila melanogaster*, we can directly measure the influence of various muscle protein isoforms and mutations on indirect flight and jump muscle performance (2,11,12). Techniques such as *P*-element-mediated transformation, along with the availability of various muscle-specific protein nulls, enable the transgenic replacement of specific proteins in selected muscles (13). The first use of the *Drosophila* system for expressing an altered version of the MHC was the transgenic expression of an embryonic (EMB) MHC in *Drosophila* indirect flight muscle (IFM). The substitution resulted in loss of flight ability (14). Subsequently, it was shown that substitution of the EMB isoform for the native IFI transformed the IFM from a high-power-generating muscle that works optimally at high oscillation frequencies to one that produces less power and functions best at low oscillation frequencies (7).

The *Drosophila* system is particularly suited for structure/function studies of MHC due to its mechanism of MHC isoform production and the wide variance in muscle fiber types. A diverse array of MHC isoforms is generated through alternative splicing of mRNA transcripts from the single copy *Mhc* gene (15–17). Fifteen isoforms have been identified to date, which are expressed in a wide variety of fiber types (18,19), including the supercontractile EMB body wall muscle and the IFM, the fastest muscle type identified to date. There are five sets of alternatively spliced exons in *Mhc*, four of which encode portions of the head region. The EMB and IFI isoforms differ at all four S-1 variable regions (Fig. 1) (20). Mapping the location of the alternative exons on an atomic-resolution, three-dimensional (3D) MHC S-1 structure directs us to a limited number of regions of the molecule that are likely to establish specific myosin properties that, presumably, are key to fiber mechanical variation (21).

Drosophila exon 9 encodes residues that correspond to amino acids 472–528 of chicken skeletal muscle MHC, a segment that is denoted the relay domain (Fig. 1). The relay domain has been implicated as an important communication pathway between the nucleotide binding site (through switch II), the actin binding site, and the lever arm via the converter

Submitted May 2, 2008, and accepted for publication August 19, 2008.

Address reprint requests to Douglas Swank, Center for Biotechnology and Interdisciplinary Studies, Rensselaer Polytechnic Institute, 110 8th St., Troy, NY 12180. Tel.: 518-276-4174; Fax: 518-276-2851; E-mail: swankd@rpi.edu.

Editor: Claudia Veigel.

0006-3495/08/12/5228/10 $2.00

doi: 10.1529/biophysj.108.136192

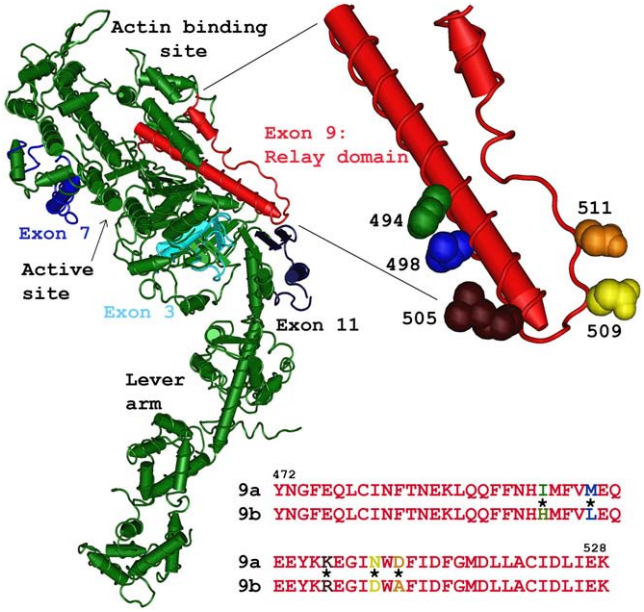

FIGURE 1 Location and two alternative sequences of the *Drosophila* relay domain region. The relay domain (exon 9, *red*) and the three other variable regions (3, 7, and 11) encoded by *Drosophila* alternative exons (*shades of blue*) are mapped onto the chicken myosin S1 structure (*green*). The relay domain spans from the end of switch II, down toward the converter (*dark blue*), and back up toward the actin-binding site. The magnified region shows the position of the five amino acids in the relay that differ between the EMB and IFI myosin isoforms. The five amino acids shown are those of chicken skeletal muscle myosin, as the structure of *Drosophila* myosin has not been determined. The IFI (9a) and EMB (9b) alternative amino acid sequences are shown below the molecular structure. The color of the amino acid single letter corresponds to the space-filling amino acid in the relay magnified region; * signifies residues that are different between 9a and 9b.

region (22–25). There are three alternative choices for exon 9: 9a, 9b, and 9c. Whereas exon 9 encodes 57 amino acids, there are only five specific amino acid differences between the IFI and EMB versions (Fig. 1). The IFI version, 9a, is expressed only in two adult muscles. These two adult muscles, the IFM and the tergal depressor of the trochanter (TDT), also called the jump muscle, are likely the two fastest muscle types found in *Drosophila* (19). The EMB version, 9b, is expressed in the remainder of the adult muscles, in embryoni and larval intermediate and internal body wall muscles, visceral muscles, and embryoni cardioblasts. Version 9c is found primarily in external embryoni body wall muscles.

Our previous exchange of relay domains between the IFI and EMB myosin isoforms altered myosin molecular properties in an unusual manner compared to our three other alternative exon exchanges (26). This exchange created two myosin chimeras, referred to as IFI-9b (IFM isoform with the EMB version of the relay domain) and EMB-9a (the EMB isoform with the IFI version of the relay domain). IFI-9b myosin showed no difference in motility or ATPase rates compared to IFI myosin. However, EMB-9a decreased actin-activated Mg^{2+}ATPase rate by 60%, increased actin affinity (K_m), and abolished actin movement in the in vitro motility assay compared to EMB myosin (26). We suggest that a decrease in myosin cross-bridge transition rates involving a state in which actin is strongly bound slows EMB-9a kinetics.

To define the influence of the relay domain at the muscle fiber level and determine how the decreased function of EMB-9a affects muscle performance, we measured sinusoidal power generation properties of IFM fibers expressing the two exon 9 myosin chimeras. IFI-9b active stiffness, work, and power generation were decreased and fiber kinetics slowed compared to IFI fibers. These observations were consistent with a reduced flight performance of flies expressing IFI-9b in their IFM. Surprisingly, EMB-9a fibers were not only fully functional under sinusoid conditions, but power levels were higher and muscle kinetics faster compared to EMB fibers. We suggest that the EMB-9a exchange creates a myosin isoform where the cross-bridge cycle is unable to effectively proceed beyond a load-sensitive step of the cycle under unloaded or near-unloaded conditions, such as in the motility assay. However, the imposed oscillatory load during sinusoidal mechanical perturbations enables myosin to overcome this raised energy barrier. Based on the combined results from both chimeras, we propose that the IFI relay increases actomyosin kinetics in response to load, whereas the EMB relay is much less responsive to load.

MATERIALS AND METHODS

The EMB and the IFI (also referred to as pWMhc2) transgenic lines were produced by *P*-element-mediated transformation, as described previously (2,14). Cloning and construction of lines expressing the exon 9 chimeras were performed as described previously (26). Transgenes were inserted into the *Drosophila* germline by *P*-element-mediated transformation (13). Reverse transcription polymerase chain reaction (RT-PCR) and sodium dodecyl sulfate polyacrylamide gel electrophoresis (SDS-PAGE) confirmed that all transgenes properly expressed the expected protein (26).

To control for the possibility that the transgenes inserted into a gene that is important for IFM function, we tested multiple lines that were each generated from independent transgene insertions into the genome. We mechanically evaluated two EMB-9a lines and observed statistically identical results (Tables 1 and 2). Similarly, we mechanically evaluated fibers from two IFI-9b lines that performed similarly and maximally in flight tests (Table 3). No significant differences were observed between each set of two lines (Tables 1 and 2). We have previously shown that the IFI line used in this study is mechanically identical to a separately generated IFI line (7,10). Similarly, the EMB line is mechanically identical to a second EMB line (10). The IFI and EMB control data for this study were generated from new experiments.

Mechanics protocol

Mechanical evaluation of fibers was performed as previously described (6,10). In brief, a bundle of six IFM fibers was dissected from a half thorax. The IFI and IFI-9b fibers were from 2–3-day-old flies, whereas the EMB and EMB-9a fibers were from flies gathered immediately after eclosion from the pupal case to not more than 2 h after eclosion. Fibers were separated and a single fiber was split lengthwise, producing a preparation ~130 μm in diameter and ~600 μm in length. Fibers were chemically demembranated (skinned) in a relaxing solution (5 mM MgATP, 15 mM creatine phosphate, 240 U/mL creatine phosphokinase, 1 mM free Mg^{2+}, 5 mM EGTA, 20 mM N,N-Bis(2-hydroxyethyl)-2-aminoethanesulfonic acid (pH 7.0), 200 mM

TABLE 1 Summary of dynamic properties

	N	Complex stiffness (kN m^{-2})	$-E_v$ (kN m^{-2})	fE_v (Hz)	E_e (kN m^{-2})	P_{max} (W m^{-3})	f_{max} (Hz)	r_3 (s^{-1})
IFI	11	366 ± 28	159 ± 9	112 ± 6	332 ± 28	96 ± 7	131 ± 5	1133 ± 54
IFI-9b, 1	12	258 ± 18*	115 ± 10*	83 ± 6*	236 ± 15*	54 ± 7*	104 ± 6*	NA
IFI-9b, 3	12	268 ± 25*	133 ± 19	85 ± 3*	255 ± 24*	49 ± 6*	117 ± 4*	910 ± 39*
EMB	12	65 ± 5	28 ± 3	20 ± 0.4	59 ± 4	2.4 ± 0.2	20 ± 0.2	98 ± 4
EMB-9a, 18	11	114 ± 10†	68 ± 5†	24 ± 0.9†	94 ± 9†	7.4 ± 0.4†	26 ± 0.7†	137 ± 4†
EMB-9a, 34	7	79 ± 13	46 ± 6†	26 ± 0.7†	66 ± 11	5.1 ± 0.9†	28 ±1.0 †	156 ± 5†

Complex stiffness and elastic modulus (E_e) values for IFI and IFI-9b were measured at the frequency (f_{max}) at which IFI generated maximum power (P_{max}). E_e and complex stiffness values for EMB and EMB-9a were measured at the specific f_{max} of each fiber type. fE_v is the average frequency at which the viscous modulus amplitude was lowest. $-E_v$ is the average minimum amplitude for the viscous modulus. r_3 is the rate constant for phase 3 of force recovery after a quick lengthening step (see Materials and Methods). EMB-9a, 34 is a second EMB-9a line created by an independent transformation event. IFI-9b, 3 is a second IFI-9b line created by an independent transformation event. All values are mean ± SE.
*Statistically different from IFI (*t*-test, $p < 0.05$).
†Statistically different from EMB (*t*-test, $p < 0.05$).

ionic strength, adjusted with Na methane sulfonate, 1 mM DTT, and 50% glycerol) containing 0.5% Triton X-100, for 1 h at 4°C. T-clips, laser cut from food-grade aluminum foil (from MicroConnex, Snoqualmie, WA) were used to mount the fibers on a mechanics rig (27), and the temperature was set at 15°C. A fiber was stretched until just taut and then lengthened by 1% muscle length increments until it reached 5% over just taut length. Sinusoidal analysis (see next paragraph) was performed while the fiber was in relaxing solution. The fiber was activated to pCa 5.0 by three partial solution exchanges of the initial relaxing solution with activating solution (same as relaxing solution, but with calcium content adjusted to pCa 4.0). Sinusoidal analysis was performed in activating solution. The fiber was stretched by 2% muscle length increments until work output, as determined by sinusoidal analysis, was maximal (typically requiring a further stretch of 6% beyond the length to which the fiber was initially stretched before activation). Tension was measured and a step analysis was performed at this optimal length. The relaxing solution was then exchanged into the chamber, tension was measured, and step and sinusoidal analyses were repeated. High calcium rigor tension was measured at the end of the experiment by replacing activating solution with a bathing solution of activating solution minus ATP, creatine phosphokinase, and creatine phosphate.

Sinusoidal analysis

Sinusoidal analysis was performed to determine muscle mechanical properties, as previously described (7,27). Briefly, sinusoidal length changes of 0.25% muscle length (peak to peak) were applied over 47 frequencies from 1 to 1000 Hz to the fiber. For each frequency, the elastic and viscous moduli were calculated from the length and tension transients by computing the amplitude ratio and the phase difference for the change in tension and length at each frequency. Work (Jm^{-3}) = $\pi E_v (\Delta L/L)^2$ and Power (Wm^{-3}) = $\pi f E_v (\Delta L/L)^2$, where f is the frequency of the length perturbations (s^{-1}), E_v is the viscous modulus at f, and $\Delta L/L$ is the amplitude of the sinusoidal length change divided by the length of the fiber between the two T-clips.

TABLE 2 Isometric properties

	Number	T_{max} (mN/mm^2)	Passive tension (mN/mm^2)	Rigor tension (mN/mm^2)
IFI	11	0.9 ± 0.2	2.1 ± 0.2	2.9 ± 0.5
IFI-9b, 1	12	1.7 ± 0.3*	1.8 ± 0.1	2.5 ± 0.3
IFI-9b, 3	12	1.6 ± 0.2*	1.5 ± 0.2	2.3 ± 0.4
EMB	12	0.49 ± 0.07	0.46 ± 0.10	0.57 ± 0.09
EMB-9a, 18	12	1.25 ± 0.21*	0.59 ± 0.11	1.28 ± 0.21*
EMB-9a, 34	7	0.88 ± 0.16*	0.43 ± 0.05	1.23 ± 0.24*

T_{max}, net active tension (gross active tension minus passive tension); Rigor tension, net rigor tension (gross rigor tension minus passive tension); EMB-9a, 34 is a second EMB-9a line created by an independent transformation event; IFI-9b,3 is a second IFI-9b line created by an independent transformation event. All values are mean ± SE.
*Statistically different from EMB (*t*-test, $p < 0.05$).

Step analysis

Step analysis was performed as previously described (6,10). To determine the rate of tension redevelopment (r_3), activated fibers were subjected to a series of four identical 0.5% muscle-lengthening steps. The force response was averaged over the four steps. The force response after the initial spike, Huxley-Simmons phases 2–4, was fit to the sum of three exponential curves: $a_1[1-\exp(-k_1 t)] + a_2\exp(-k_2 t) + a_3\exp(-k_3 t)$ + offset. Constants a_1, a_2, a_3 are amplitudes; k_1, k_2, and k_3 are rate constants; k_1 is r_3 (phase 3), the only increasing term with time and the second fastest rate of the three; k_2 is the fastest, the initial force decline (phase 2); and k_3 is the slow decline after force recovery (phase 4). The offset adjusts for nonzero starting values. The motor response time for each step was <0.5 ms.

Flight assays

Wing-beat frequency (WBF) and flight ability were measured at 22°C and at 15°C, the temperature at which muscle mechanical measurements were performed, to allow direct comparison of muscle kinetics and flight parameters. The WBF of a tethered fly was determined using an optical tachometer (28). Flight ability was assayed by observing whether a fly was capable of flying up (U), horizontal (H), down (D), or not at all (N) when released in a Plexiglas flight chamber (29). The flight index equals $6U/T + 4H/T + 2D/T + 0N/T$, where T is the total number of flies tested (30).

Electron microscopy

To determine the ultrastructure stability of transgenic myofibrils, we observed the structure of less than 2-h-old EMB and EMB-9a fibers. We

TABLE 3 Flight characteristics

	Flight index, 22°C	WBF, 22°C	Flight index, 15°C	WBF, 15°C
IFI	4.4 ± 0.3 (42)	172 ± 3 (15)	2.9 ± 0.1 (108)	157 ± 2 (8)
IFI-9b, 1	4.4 ± 0.3 (61)	167 ± 3 (14)	2.7 ± 0.1 (129)	143 ± 1 (18)*
IFI-9b, 3	4.8 ± 0.2 (54)	169 ± 4 (13)	2.5 ± 0.1 (88)*	143 ± 1 (18)*

All values are mean ± SE. Number of flies tested is in parentheses. IFI-9b, 1, and 3 are independently generated, transgenic IFI-9b lines.
*Statistically different from IFI (*t*-test, $p < 0.05$).

previously showed that IFI-9b fibers were ultrastructurally identical to IFI fibers (26). Details of electron microscopy, fixation, osmium staining, embedding, and thin sectioning were as previously described (31).

RESULTS

Ultrastructure of transgenic fibers

We used transmission electron microscopy to evaluate the ultrastructure of the transgenic fibers to assess the reliability of mechanical values, particularly those dependent on cross-sectional area. The IFI-9b ultrastructure is identical to the IFI control ultrastructure (26); therefore, the IFI-9b ultrastructure has no impact on the mechanical performance of the fibers. However, EMB-9a fibers show considerable ultrastructure disarray, even at less than 2 h of age (Fig. 2, *B* and *C*). The disarray was substantially worse than the minor disarray seen with EMB expressing fibers, which usually display only a few misshapen myofibrils or an occasional missing thick or thin filament at less than 2 h of age (Fig. 2 *A*). This is unusual compared to our other EMB chimeras (EMB-IC, EMB-7d, and EMB-3b) that showed a normal ultrastructure or an ultrastructure equivalent to the EMB ultrastructure at 2 h of age (6,7,10). Previously, studies with these chimeras yielded highly reproducible mechanical data; therefore, all mechanical measures of EMB-9a that involve normalization to cross-sectional area should be viewed as having a higher degree of uncertainty than our previous work with the other EMB chimeras.

The diameter of 2-h-old *Drosophila* myofibrils is less than that of 2-day-old myofibrils, as IFM development continues with additional thick and thin filament accumulation for at least several hours after eclosion (32). In young fibers, the reduced number of filaments per fiber cross-sectional area results in lower power, tension, and work values, as evident from our previous experiments on less than 2-h-old IFI control fibers (denoted as IFI-2h in Swank et al. (10)) compared to 2-day-old IFI fibers. Thus, any mechanical values that are normalized to fiber cross-sectional area should only be compared to fibers of a similar age. In contrast, the kinetics of IFI and IFI-2h were similar. For that reason, kinetic properties, such as the frequency of maximum power generation (f_{max}) (Table 1) (10), can be compared across all ages.

Mechanical analysis of transgenic IFM fibers

Complex stiffness and phase

To determine whether exchanging relay domains between IFI and EMB myosin affected muscle mechanical and kinetic properties, we employed small-amplitude sinusoidal analysis. The complex stiffness amplitude of IFI-9b fibers was significantly reduced compared to IFI fiber complex stiffness over almost all frequencies tested (Fig. 3 *A*). A decrease to 73% of IFI complex stiffness was observed at the frequency at which maximum power was generated (f_{max}) (Table 1). The phase plot for IFI-9b fibers was shifted to the left compared to IFI, signifying a slowing in overall fiber kinetics (Fig. 3 *A*).

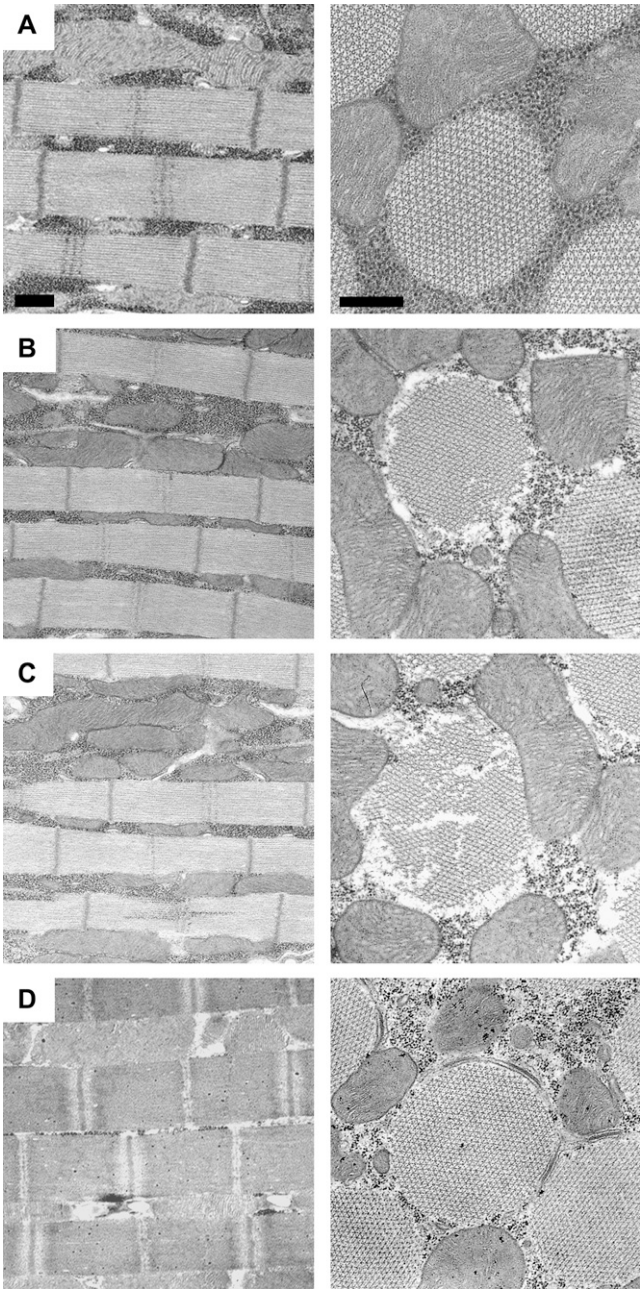

FIGURE 2 IFM myofibril ultrastructure. All panels display longitudinal (*left*) and transverse (*right*) views of dorsolongitudinal muscles (the medial set of the two opposing sets of IFMs). Scale bars: 0.5 μm. Flies were less than 2 h post eclosion. (*A*) EMB-IFMs exhibit minimal ultrastructural abnormalities, as previously reported (6,10). (*B*) EMB-9a IFM myofibril ultrastructure. This example has above-average quality ultrastructure for EMB-9a fibers. (*C*) A more typical region of EMB-9a fiber showing regions of missing thick and thin filaments, and myofibrils that are not uniform in width. (*D*) IFI (control) fiber showing the typical, highly ordered ultrastructure of *Drosophila* IFM myofibrils.

An opposite trend was observed for EMB-9a, with EMB-9a complex stiffness amplitude being higher than that of

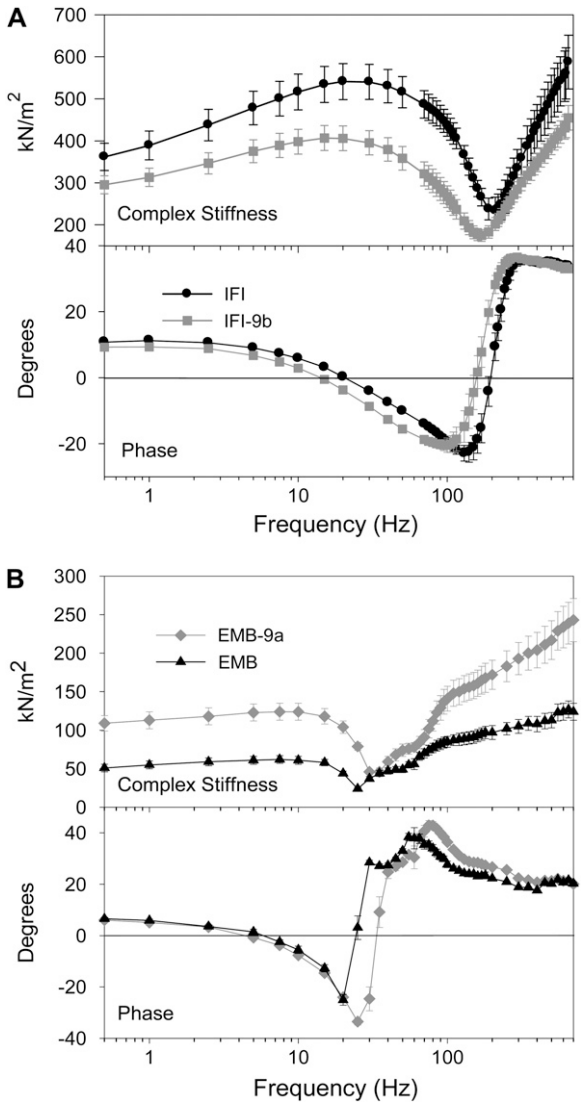

FIGURE 3 Complex stiffness and phase shift of maximally Ca^{2+}-activated IFM fibers at 15°C. (*A*) Complex stiffness and phase as a function of frequency for IFI and IFI-9b IFM fibers from 2-day-old flies. (*B*) Complex stiffness and phase as a function of frequency for EMB-9a and EMB fibers from less than 2-h-old adults. Note the different *y*-axis scales for complex stiffness in panels *A* and *B*, as fibers from the younger flies have less myofibril area per cross section (see text).

EMB at almost all frequencies tested (Fig. 3 *B*). EMB-9a complex stiffness amplitude was ~1.2-fold higher at f_{max} (Table 1). At most frequencies, the complex stiffness was over twofold higher. The EMB-9a phase plot was shifted to the right, indicating an overall increase in speed of fiber kinetics compared to EMB (Fig. 3 *B*).

Elastic and viscous moduli

We determined which differences in complex stiffness are due to active force-generating or force-absorbing processes (viscous modulus), and which are primarily due to differences in passive muscle elements (elastic modulus) by separating fiber complex stiffness into its elastic and viscous components (Fig. 4). A leftward shift of IFI-9b's minimum elastic and viscous moduli amplitudes to lower frequencies was observed compared to IFI moduli (Fig. 4, A and B), indicating that IFI-9b myosin kinetics are better suited for lower muscle oscillation frequencies than IFI myosin.

Amplitude differences between IFI and IFI-9b moduli were greater for the elastic modulus than for the viscous modulus. Elastic modulus amplitude differences were largest between 1 and 120 Hz, including a 30% decrease for IFI-9b compared to IFI fibers at 30 Hz, suggesting higher elastic compliance in the IFI-9b cross-bridge than IFI. Thus, IFI-9b fibers likely store less energy elastically than IFI fibers.

Viscous modulus comparisons between the two fiber types showed that IFI fibers had higher viscous modulus values in work-absorbing regions (above zero), whereas in work-generating regions (below zero) IFI viscous modulus values were lower than IFI-9b (Fig. 4 B). Since the muscle length change for both fibers was identical at all frequencies, the maximum work per cycle is proportional to the viscous modulus (E_v). Thus, IFI is capable of producing more work over the mid-range frequencies, and absorbing more work over the low- and high-frequency ranges. The maximum work produced by IFI fibers was 1.4-fold higher than IFI-9b ($-E_v$, Table 1). IFI-9b's frequency at which maximum work is produced was 71% of IFI's maximum frequency (fE_v; Table 1).

Comparing EMB-9a to EMB, we observed a rightward shift in both the elastic and viscous moduli (Fig. 4, *C* and *D*), suggesting that fibers expressing EMB-9a myosin operate best at faster oscillation speeds than EMB expressing fibers. EMB-9a fE_v was 1.3-fold higher than EMB. EMB-9a elastic modulus was greater (stiffer) than that of EMB at most frequencies (Fig. 4 *C*). EMB-9a viscous modulus dipped lower than EMB, revealing that EMB-9a fibers produce more work, which was confirmed by the twofold difference in minimum viscous modulus amplitude ($-E_v$) of EMB-9a and EMB fibers (Table 1). The greater viscous modulus of EMB-9a at high frequencies suggests that it is capable of absorbing more work than EMB at these frequencies (Fig. 4 *D*), and the higher elastic modulus at almost all frequencies shows that EMB-9a fibers are capable of recovering more work than EMB fibers.

Power generation

The most important mechanical property of *Drosophila* IFM is power generation for flight. Power generation was significantly influenced by alternative versions of the relay domain. P_{max} for IFI-9b fibers was 56% of IFI P_{max} (Table 1) and occurred at ~110 Hz compared to 130 Hz for IFI (f_{max}; Table 1, Fig. 5). At low frequencies (20–70 Hz), power production by IFI-9b fibers was equal to IFI power production. A decrease in the power-producing ability of IFI-9b fibers compared to IFI fibers occurred over the frequency range of 75–200 Hz. IFI-9b fibers could not generate power above 160 Hz, but IFI fibers were able to generate power up to 190 Hz.

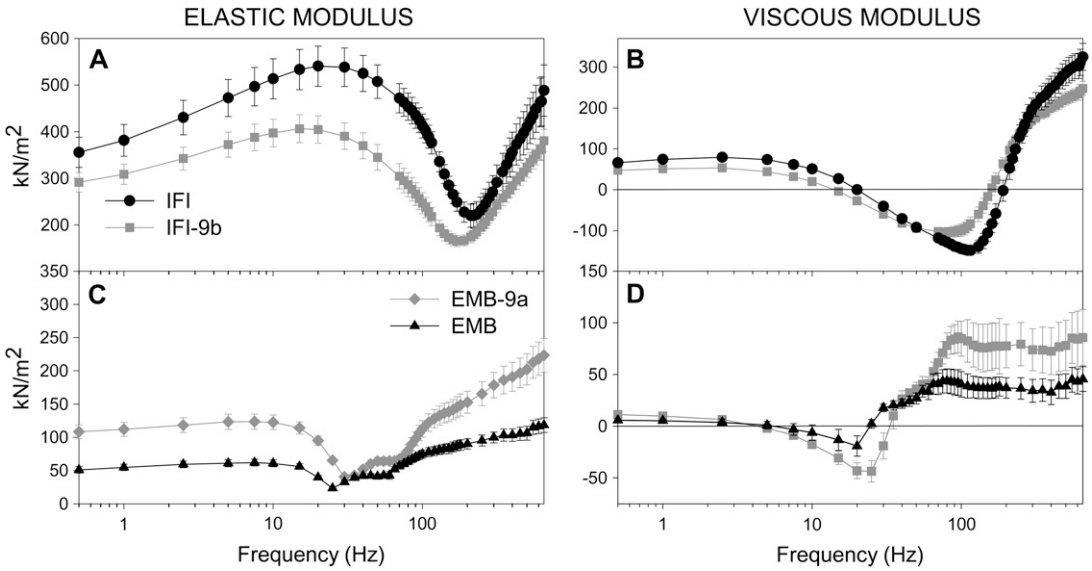

FIGURE 4 Elastic and viscous moduli of maximally Ca^{2+}-activated IFM fibers. Elastic modulus (instantaneous stiffness) (*A*) and viscous modulus (*B*) as a function of frequency for IFI and IFI-9b. Elastic modulus (*C*) and viscous modulus (*D*) as a function of frequency for EMB-9a and EMB. Note the different *y*-axis scales for EMB-9a and EMB relative to IFI and IFI-9b, as fibers from the younger flies have less myofibril area per cross section (see text).

In contrast, the IFI relay domain increased the power-generating ability of EMB fibers. P_{max} increased almost threefold, and EMB-9a frequency of maximum power generation (f_{max}) was 1.4-fold greater than EMB (Fig. 5, Table 1). EMB fibers could not generate power above 25 Hz, whereas EMB-9a generated useful power up to 35 Hz. Above 35 Hz, EMB-9a muscle was not capable of producing useful power. EMB-9a's useful frequency range was ~4-fold lower than the WBF range thought to be capable of providing sufficient aerodynamic power for *Drosophila* flight (6).

Rate of force redevelopment, r_3

Another method of measuring fiber kinetics, step analysis (33–35), confirmed our sinusoidal analysis results (Table 1). Exchanging the EMB relay domain into IFI (IFI-9b) slowed r_3 (rate of force regeneration after a lengthening step, Fig. 6) to 80% of IFI r_3. Conversely, EMB-9a r_3 increased 1.5-fold compared to EMB r_3. These results closely resembled the differences in f_{max} and fE_v observed with the sinusoidal analysis (Table 1).

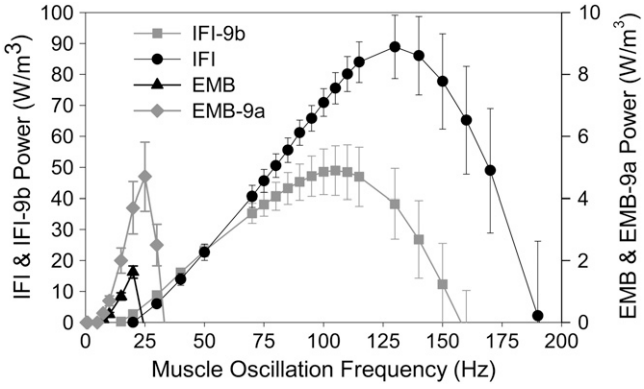

FIGURE 5 Power generation by maximally activated IFM fibers at 15°C. Power generated by IFI, IFI-9b, EMB-9a, and EMB muscle fibers when oscillated at 0.25% peak to peak strain over a frequency range of 0.5–200 Hz. Note the separate *y*-axis scale for EMB and EMB-9a versus IFI and IFI-9b. The former generate less power than the latter due to the use of much younger fibers for EMB and EMB-9a (see text). The EMB and EMB-9a power scale has been adjusted, based on a previous comparison of EMB and IFI fiber power output from less than 2-h-old flies (10), so that the relative height of all the curves approximates the relative power generation of all four fiber types, as if all fibers were from flies of the same age.

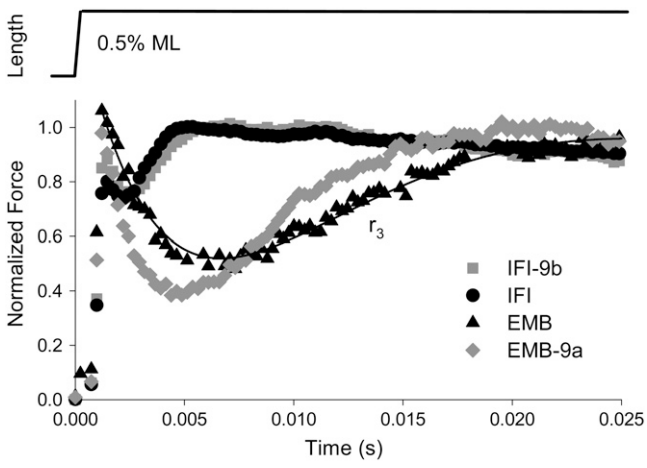

FIGURE 6 Representative tension responses to a rapid lengthening step for all four transgenic fiber types. IFM fibers at pCa 5.0 were subjected to a rapid lengthening step, 0.5% muscle length. Tension levels are normalized to maximum tension after phase 3; r_3 is the rate of tension redevelopment in phase 3. The solid line is an exemplar fit of the sum of three exponential curves to the EMB fiber force response (see Materials and Methods).

Isometric tension

Exchanging the EMB relay domain into IFI increased isometric force production, as IFI-9b net isometric tension (T_{max}) was slightly higher than IFI T_{max} (Table 2). This is logical since IFI-9b muscle kinetics were slower than IFI kinetics, suggesting that IFI-9b myosin, compared to IFI, spends a longer period of time in strongly bound states than in weakly bound states, which results in higher tension generation. However, this reasoning did not hold for EMB-9a compared to EMB. EMB-9a T_{max} was higher than EMB (Table 2), even though EMB kinetics were slower than EMB-9a (Table 1). Rigor tension was higher for EMB-9a than EMB. No differences in rigor tension were observed for IFI-9b compared to IFI. Passive tension, pCa = 8.0, was not different for either chimera compared to its appropriate control.

Flight ability

Drosophila flight performance at colder temperatures, specifically 15°C, the same temperature at which we performed the fiber mechanics study, was significantly impaired by inserting the EMB relay domain into IFI myosin. IFI-9b flight indexes dropped to 2.5 and 2.7 compared to 2.9 for IFI (Table 3, column 3). The decreased flight ability was caused, at least in part, by a slower WBF, since the WBF of IFI-9b lines was 91% of IFI WBF (Table 3, column 4) and aerodynamic power is proportional to the third power of WBF (36,37). A physiological impact of exchanging the EMB relay domain into IFI on flight was not readily apparent at warmer temperatures (22°C), where IFI-9b *Drosophila* flight index and WBF values were not statistically different from IFI values (Table 3, columns 1 and 2) (26). Neither EMB nor EMB-9a *Drosophila* could fly at any temperature. This is primarily due to an inability of muscle fibers from these lines to generate power when oscillated at frequencies corresponding to frequencies that support flight.

DISCUSSION

Our results show that alternative versions of the myosin relay domain are important in setting fundamental functional differences between *Drosophila* muscle fiber types. The two alternative relay domains affected basic mechanical properties, including work, power, kinetics of power generation, r_3, tension generation, and muscle stiffness. Although they significantly altered EMB and IFI functional properties, neither exchange completely converted IFI to EMB or vice versa. IFI power-generating kinetics are 6.5-fold faster (f_{max}) and produce 4.4-fold higher power than EMB fibers (7,10). The relay domain, at most, caused a twofold change in these two properties. The exchange did not produce exactly equal and opposite results, as the IFI relay exchange into EMB increased EMB power generation kinetics slightly more than the decrease in kinetics from the EMB relay exchange into IFI. Surprisingly, as discussed below, the fiber mechanics results for both chimeras did not correlate with changes in actin velocity and ATPase rates that we previously measured at the molecular level (26).

EMB-9a generates muscle power, but not actin motility

The ability of EMB-9a fibers to produce power under oscillatory conditions was unexpected, as our previous isolated myosin measurements showed no ability of EMB-9a myosin to move actin filaments, a decrease in actin-activated Mg^{2+}ATPase rate to 40% of EMB's rate and a decrease in K_m to 33% of EMB's K_m (26). EMB-9a muscle ultrastructure deteriorates faster than EMB ultrastructure with age, which we attributed to the slower EMB-9a cross-bridge kinetics being more deleterious to IFM function than EMB kinetics. Thus, it was surprising that EMB-9a fibers were not only functional but produced higher amounts of power at a higher f_{max} than EMB fibers. If EMB-9a fiber ultrastucture integrity had been the same as EMB, EMB-9a likely would have produced even more power compared to EMB than we measured.

We previously suggested that the lack of motility is due to EMB-9a myosin becoming trapped in a strongly actin bound state, most likely associated with ADP release or ATP binding (26). Our current observation that EMB-9a fiber isometric tension is higher than EMB tension supports this hypothesis. If myosin's rate of transition out of a strongly bound state is greatly slowed, then isometric tension would be higher because a greater number of cross-bridges would be bound to actin at any given time. However, a slowed transition involving strongly bound cross-bridges would also be expected to slow EMB-9a fiber kinetics compared to EMB kinetics under oscillatory work-producing conditions. Since we measured faster fiber kinetics for EMB-9a compared to EMB, we need to examine the basis of increased myosin kinetics during oscillatory work production, but not under static isometric tension conditions or during the actin motility assay.

Myosin working in a fully active muscle fiber differs from its performance in the motility assay. In muscle, myosin operates in a constrained lattice, thin filament binding proteins are present, and myosin experiences a significant load. Whereas geometry and thin filament proteins can alter motility velocity (20,38), their absence should not cause a complete stoppage of actin in vitro motility. There is ample fiber mechanical evidence that muscle kinetics are sensitive to load (39,40). Positive load has been postulated to be critical for how the fastest known nonmuscle myosin, from *Chara*, is able to achieve its extremely high actin velocity (41). Huxley and Simmons (42) proposed a model for the effect of load, where cross-bridges under low load proceed through their load-sensitive states rapidly, whereas under high load they go through these states much more slowly.

Recent sophisticated optical trapping studies using a three-bead assay and sinusoidal perturbations provided direct

evidence for load-sensitive cross-bridge states at the single-molecule level. Veigel et al. (43) confirmed the Huxley-Simmons model by finding that load influences the length of time smooth muscle myosin spends bound to actin. ADP release kinetics of smooth muscle myosin are accelerated by an assistive load and slowed with a resistive load (44). Kad et al. (44) also observed that load can partially restore function to a smooth muscle myosin mutant, glycine 709 (699 skeletal) to valine, which abolishes movement in the actin motility assay. This mutant residue is located in the SH1-SH2 helix and is thought to interact with the relay helix. The lack of function in the motility assay is due to decreased ADP release and ATP binding rates (44). As with wild-type smooth muscle myosin, an assistive load increased ADP release rate of the mutant; however, both an assistive and a resistive load accelerated ATP binding of the mutant by 20-fold.

Since significant differences between the IFI and EMB relay are located near the region thought to interact with amino acid 699 (44) and our exchange showed a very similar phenotype to the 699 mutant, a similar mechanism may be responsible for EMB-9a's phenotype. A general explanation may be that the IFI relay domain in the EMB myosin background raises the activation energy barrier between two cross-bridge states that, in the absence of significant load (i.e., in the motility assay), cannot be overcome. However, the addition of assistive and/or resistive load on myosin when the EMB-9a fiber is oscillated by the servomotor lowers this energy barrier, or provides additional energy to overcome the barrier. If correct, this suggests that the relay domain is a myosin load sensor and that the isoform-specific amino acids differentially affect load sensitivity.

IFI-9b slows muscle fiber kinetics, but not in vitro actin velocity

In contrast to EMB-9a, IFI-9b myosin decreased IFM power-generating ability and slowed IFM kinetics. However, we measured no differences in actin-activated Mg^{2+}ATPase, Ca^{2+}ATPase, or actin motility velocity between IFI-9b and IFI myosin (26). This result is unusual, as our studies of other EMB exons exchanged into IFI found that if a decrease in muscle fiber kinetics occurred, the decrease correlated with either a decrease in actin-activated Mg^{2+}ATPase rate and/or a decrease in actin motility velocity (6,7,10). The reason for the current lack of correlation may again be due to different conditions myosin experiences in the motility assay compared to muscle. We propose that response to load explains this observation. By exchanging the EMB relay into IFI, IFI lost some sensitivity to load, thus decreasing strongly bound transition rates in the cross-bridge cycle.

The combined mechanical evaluation of EMB-9a and IFI-9b fibers and myosin suggests that the IFI relay is more effective at responding to load or transmitting intermolecular strain that leads to increased cross-bridge kinetics. In contrast, the EMB relay is less effective at transmitting strain or responding to load to increase rates of work-producing transitions, resulting in slower kinetics. This mechanism suggests that IFI myosin may store negative stress near the end of muscle lengthening, which is returned during shortening. The IFI cross-bridge may have a higher spring constant than EMB due in part to its specific relay domain. The higher elastic modulus of EMB-9a compared to EMB, and the higher elastic modulus of IFI compared to IFI-EC support this hypothesis. Such a mechanism would be energetically and perhaps mechanically advantageous for an oscillatory power production system, which needs higher force generation during shortening than lengthening to generate work and power.

Potential differences in relay load sensitivity could be tested with other fly muscle types. For instance, one could express myosin with different relay domains in the TDT muscle, which can be used to measure shortening under different amounts of load (45). If our hypothesis is correct, unloaded TDT fibers expressing EMB-9a should have greatly reduced shortening velocity compared to EMB fibers. At the molecular level, the three-bead optical trap (as in Kad et al. (44)), could be used to directly test the load response of *Drosophila* myosin relay chimeras.

Drosophila relay domain structural differences

Exon 9 encodes amino acids 472–528 (chicken skeletal numbering), but the only difference between the two *Drosophila* relay versions we examined were five amino acids located between 494 and 511: I494H, M498L, K505R, N509D, and D511A (9a and 9b, respectively) (Fig. 1) (21). The I494H difference is intriguing because it appears to be the only one of the five that interacts directly with another amino acid, specifically Phe-671 (Dicty 652), in two static crystal structures examined (26). However, any of the other four amino acids could also potentially affect the ability of the relay helix to adopt different conformations (23). We previously suggested that Ile-494 (Dicty 485) would interact more strongly with Phe-671 because it is more hydrophobic than His-494. Phe-671 is thought to be where the relay helix's pivoting and ''kinking'' conformational change during the cross-bridge cycle occurs (22,46). The relay helix is in a kinked form in crystal structures thought to correspond to the prepower stroke state (46,47). The relay is in a straighter conformation in crystal structures thought to correspond to the postpower stroke state (47). These conformational changes occur due to communication with the nucleotide binding site through switch II, and with the lever arm via the converter region (48,49). Load on the lever arm could be directly transferred to the relay through strain in the converter, affecting the relay's rate of transition into or out of the kinked conformation. Thus, altering the relay amino acid sequence likely alters the effectiveness of myosin intermolecular strain communication and structural rearrangement needed to proceed through the cross-bridge cycle.

Influence of the relay domain on *Drosophila* flight ability

The decrease in power generation produced by exchanging the EMB relay domain into IFI is physiologically significant as evidenced by the decrease in flight ability and WBF of IFI-9b flies compared to IFI flies at 15°C (Table 3). The reduction in WBF may be a response to the slower IFI-9b muscle kinetics. Slowed WBF would increase muscle power generation, since muscle power increases with decreasing muscle oscillation frequency over this frequency range (Fig. 5). As discussed previously (7,10), this decrease could be voluntary through the nervous system or involuntary due to changes in muscle stiffness and/or kinetics. Although it increases muscle power, the decrease in WBF sacrifices aerodynamic power ($P_{aero} \approx WBF^3$ (36)) at 15°C, accounting for the decreased IFI-9b flight index. EMB-9a and EMB *Drosophila* cannot fly due to their inability to generate power at the frequencies required to support flight.

The relative influence of all four alternative exons on IFI and EMB fiber mechanics

We have now examined the influence of all four of the S-1 alternative exon regions on IFM fiber mechanical properties. By testing the effect of each of the four EMB versions on IFI kinetics, we found that the EMB converter (encoded by exon 11c) has the greatest influence, causing a 50% decrease in IFI power-producing kinetics (f_{max}) (7,50). The EMB relay domain (encoded by exon 9b) and the EMB N-terminal region (encoded by exon 3a) both cause a 20% decrease in f_{max} (10). EMB exon 7a, which encodes a region in the nucleotide-binding pocket, did not affect IFI power-generation kinetics (6). The exchanges into IFI that decreased muscle power-generation kinetics had a negative effect on *Drosophila* flight ability. Of interest, exchanging the exon 3a EMB domain into IFI had a greater than expected negative impact on flight relative to its moderate decrease in IFM kinetics (10). Perhaps this is because 3a is the only EMB exon that decreases IFI actin-activated Mg^{2+}ATPase rate (51).

The reverse exchanges, in which the IFI alternative versions were inserted into EMB and expressed in IFM fibers, revealed that the IFI converter (exon 11e) had the greatest influence, with a 2.2-fold increase in muscle power kinetics (f_{max}) compared to IFM expressing EMB (7,50). The other three IFI exons (3b, 7d, and 9a) increased EMB f_{max} 1.7-, 1.5- and 1.4-fold (10,6). Interestingly, of the four, only the exon 7 region increased EMB kinetics without its converse exchange decreasing IFI kinetics (6). None of the IFI exchanges into EMB rescued flight ability, as the increase in kinetics by one exon exchange alone did not bring muscle power kinetics back into the range that supports flight.

None of the chimeric myosins created by exchanging alternative exons has been directly tested for the influence of load on rates of cross-bridge transitions. The alternative domains that have the greatest effect on muscle rate constants are located in areas likely to be subjected to strain: the converter region, the relay domain, and the N-terminal domain (exon 3). These regions are all near the pivot point of the lever arm. Our current results with alternative relay domains encoded by exon 9 suggest that myosin's response to load is a major determinant of how muscle kinetics are set by different myosin isoforms.

The authors thank Catherine Eldred, Joan Braddock, and Rich Lachapelle for excellent technical assistance, and Edward Pate for helpful discussions on myosin structure. This study was supported by the American Heart Association Scientist Development Grant 0635058N and National Institutes of Health grants AR055611 to D.M.S., AR049425 to D.W.M., and GM32443 to S.I.B.

REFERENCES

1. Lowey, S., G. S. Waller, and K. M. Trybus. 1993. Function of skeletal muscle myosin heavy and light chain isoforms by an in vitro motility assay. *J. Biol. Chem.* 268:20414–20418.
2. Swank, D. M., L. Wells, W. A. Kronert, G. E. Morrill, and S. I. Bernstein. 2000. Determining structure/function relationships for sarcomeric myosin heavy chain by genetic and transgenic manipulation of *Drosophila*. *Microsc. Res. Tech.* 50:430–442.
3. Murphy, C. T., and J. A. Spudich. 2000. Variable surface loops and myosin activity: accessories to a motor. *J. Muscle Res. Cell Motil.* 21: 139–151.
4. Krenz, M., A. Sanbe, F. Bouyer-Dalloz, J. Gulick, R. Klevitsky, T. E. Hewett, H. E. Osinska, J. N. Lorenz, C. Brosseau, A. Federico, N. R. Alpert, D. M. Warshaw, M. B. Perryman, S. M. Helmke, and J. Robbins. 2003. Analysis of myosin heavy chain functionality in the heart. *J. Biol. Chem.* 278:17466–17474.
5. Rovner, A. S., Y. Freyzon, and K. M. Trybus. 1997. An insert in the motor domain determines the functional properties of expressed smooth muscle myosin isoforms. *J. Muscle Res. Cell Motil.* 18:103–110.
6. Swank, D. M., J. Braddock, W. Brown, H. Lesage, S. I. Bernstein, and D. W. Maughan. 2006. An alternative domain near the ATP binding pocket of *Drosophila* myosin affects muscle fiber kinetics. *Biophys. J.* 90:2427–2435.
7. Swank, D. M., A. F. Knowles, J. A. Suggs, F. Sarsoza, A. Lee, D. W. Maughan, and S. I. Bernstein. 2002. The myosin converter domain modulates muscle performance. *Nat. Cell Biol.* 4:312–317.
8. Babu, G. J., E. Loukianov, T. Loukianova, G. J. Pyne, S. Huke, G. Osol, R. B. Low, R. J. Paul, and M. Periasamy. 2001. Loss of SM-B myosin affects muscle shortening velocity and maximal force development. *Nat. Cell Biol.* 3:1025–1029.
9. Krenz, M., S. Sadayappan, H. E. Osinska, J. A. Henry, S. Beck, D. M. Warshaw, and J. Robbins. 2007. Distribution and structure-function relationship of myosin heavy chain isoforms in the adult mouse heart. *J. Biol. Chem.* 282:24057–24064.
10. Swank, D. M., W. A. Kronert, S. I. Bernstein, and D. W. Maughan. 2004. Alternative N-terminal regions of *Drosophila* myosin heavy chain tune muscle kinetics for optimal power output. *Biophys. J.* 87: 1805–1814.
11. Peckham, M., J. E. Molloy, J. C. Sparrow, and D. C. S. White. 1990. Physiological properties of the dorsal longitudinal flight muscle and the tergal depressor of the trochanter muscle of *Drosophila melanogaster*. *J. Muscle Res. Cell Motil.* 11:203–215.
12. Maughan, D. W., and J. O. Vigoreaux. 1999. An integrated view of insect flight muscle: genes, motor molecules, and motion. *News Physiol. Sci.* 14:87–92.
13. Cripps, R. M., and S. I. Bernstein. 2000. Generation of transgenic *Drosophila melanogaster* by *P* element-mediated germline transfor-

mation. *In* Introducing DNA into Living Cells and Organisms. P. A. Norton and L. F. Steel, editors. BioTechniques Books, Eaton Publishing, Natick, MA.

14. Wells, L., K. A. Edwards, and S. I. Bernstein. 1996. Myosin heavy chain isoforms regulate muscle function but not myofibril assembly. *EMBO J.* 15:4454–4459.
15. Bernstein, S. I., K. Mogami, J. J. Donady, and C. P. Emerson, Jr. 1983. *Drosophila* muscle myosin heavy chain encoded by a single gene in a cluster of muscle mutations. *Nature.* 302:393–397.
16. Rozek, C. E., and N. Davidson. 1983. *Drosophila* has one myosin heavy-chain gene with three developmentally regulated transcripts. *Cell.* 32:23–34.
17. George, E. L., M. B. Ober, and C. P. Emerson. 1989. Functional domains of the *Drosophila melanogaster* muscle myosin heavy-chain are encoded by alternatively spliced exons. *Mol. Cell. Biol.* 9:2957–2974.
18. Hastings, K. E., and C. P. Emerson, Jr. 1982. cDNA clone analysis of six co-regulated mRNAs encoding skeletal muscle contractile proteins. *Proc. Natl. Acad. Sci. USA.* 79:1553–1557.
19. Zhang, S., and S. I. Bernstein. 2001. Spatially and temporally regulated expression of myosin heavy chain alternative exons during *Drosophila* embryogenesis. *Mech. Dev.* 101:35–45.
20. Swank, D. M., M. L. Bartoo, A. F. Knowles, C. Iliffe, S. I. Bernstein, J. E. Molloy, and J. C. Sparrow. 2001. Alternative-exon-encoded regions of *Drosophila* myosin heavy chain modulate ATPase rates and actin sliding velocity. *J. Biol. Chem.* 276:15117–15124.
21. Bernstein, S. I., and R. A. Milligan. 1997. Fine tuning a molecular motor: the location of alternative domains in the *Drosophila* myosin head. *J. Mol. Biol.* 271:1–6.
22. Mesentean, S., S. Koppole, J. C. Smith, and S. Fischer. 2007. The principal motions involved in the coupling mechanism of the recovery stroke of the myosin motor. *J. Mol. Biol.* 367:591–602.
23. Yengo, C. M., L. R. Chrin, A. S. Rovner, and C. L. Berger. 2000. Tryptophan 512 is sensitive to conformational changes in the rigid relay loop of smooth muscle myosin during the MgATPase cycle. *J. Biol. Chem.* 275:25481–25487.
24. Dominguez, R., Y. Freyzon, K. M. Trybus, and C. Cohen. 1998. Crystal structure of a vertebrate smooth muscle myosin motor domain and its complex with the essential light chain: visualization of the pre-power stroke state. *Cell.* 94:559–571.
25. Holmes, K. C., R. R. Schroder, H. L. Sweeney, and A. Houdusse. 2004. The structure of the rigor complex and its implications for the power stroke. *Philos. Trans. R. Soc. Lond. B Biol. Sci.* 359:1819–1828.
26. Kronert, W. A., C. M. Dambacher, A. F. Knowles, D. M. Swank, and S. I. Bernstein. 2008. Alternative relay domains of *Drosophila melanogaster* myosin differentially affect ATPase activity, *in vitro* motility, myofibril structure and muscle function. *J. Mol. Biol.* 379:443–456.
27. Dickinson, M. H., C. J. Hyatt, F.-O. Lehmann, J. R. Moore, M. C. Reedy, A. Simcox, R. Tohtong, J. O. Vigoreaux, H. Yamashita, and D. W. Maughan. 1997. Phosphorylation-dependent power output of transgenic flies: an integrated study. *Biophys. J.* 73:3122–3134.
28. Hyatt, C. J., and D. W. Maughan. 1994. Fourier analysis of wing beat signals: assessing the effects of genetic alterations of flight muscle structure in *Diptera*. *Biophys. J.* 67:1149–1154.
29. Drummond, D. R., M. Peckham, J. C. Sparrow, and D. C. S. White. 1990. Alteration in crossbridge kinetics caused by mutations in actin. *Nature.* 348:440–442.
30. Tohtong, R., H. Yamashita, M. Graham, J. Haeberle, A. Simcox, and D. Maughan. 1995. Impairment of muscle function caused by mutations of phosphorylation sites in myosin regulatory light chain. *Nature.* 374:650–653.
31. O'Donnell, P. T., and S. I. Bernstein. 1988. Molecular and ultrastructural defects in a *Drosophila* myosin heavy chain mutant: differential effects on muscle function produced by similar thick filament abnormalities. *J. Cell Biol.* 107:2601–2612.
32. Reedy, M. C., and C. Beall. 1993. Ultrastructure of developing flight muscle in *Drosophila*. I. Assembly of myofibrils. *Dev. Biol.* 160:443–465.
33. Ford, L. E., A. F. Huxley, and R. M. Simmons. 1977. Tension responses to sudden length change in stimulated frog muscle fibres near slack length. *J. Physiol.* 269:441–515.
34. Steiger, G. J. 1977. Stretch activation and tension transients in cardiac, skeletal and insect flight muscle. *In* Insect Flight Muscle. R. T. Tregear, editor. North Holland, Amsterdam, The Netherlands. 221–268.
35. Davis, J. S., and N. D. Epstein. 2003. Kinetic effects of fiber type on the two subcomponents of the Huxley-Simmons phase 2 in muscle. *Biophys. J.* 85:390–401.
36. Laurie-Ahlberg, C. C., P. T. Barnes, J. W. Curtsinger, T. H. Emigh, B. Karlin, R. Morris, R. A. Norman, and A. N. Wilton. 1985. Genetic variability of flight muscle metabolism in *Drosophila melanogaster*. II. Relationship between power output and enzyme activity levels. *Genetics.* 111:845–868.
37. Dickinson, M. 2001. Solving the mystery of insect flight. *Sci. Am.* 284:48–57.
38. Gordon, A. M., E. Homsher, and M. Regnier. 2000. Regulation of contraction in striated muscle. *Physiol. Rev.* 80:853–924.
39. Fenn, W. O. 1923. A quantitative comparison between the energy liberated and the work performed by the isolated sartorius muscle of the frog. *J. Physiol.* 58:175–203.
40. Cooke, R. 1997. Actomyosin interaction in striated muscle. *Physiol. Rev.* 77:671–697.
41. Kimura, Y., N. Toyoshima, N. Hirakawa, K. Okamoto, and A. Ishijima. 2003. A kinetic mechanism for the fast movement of *Chara* myosin. *J. Mol. Biol.* 328:939–950.
42. Huxley, A. F., and R. M. Simmons. 1971. Proposed mechanism of force generation in striated muscle. *Nature.* 233:533–538.
43. Veigel, C., J. E. Molloy, S. Schmitz, and J. Kendrick-Jones. 2003. Load-dependent kinetics of force production by smooth muscle myosin measured with optical tweezers. *Nat. Cell Biol.* 5:980–986.
44. Kad, N. M., J. B. Patlak, P. M. Fagnant, K. M. Trybus, and D. M. Warshaw. 2007. Mutation of a conserved glycine in the SH1–SH2 helix affects the load-dependent kinetics of myosin. *Biophys. J.* 92: 1623–1631.
45. Yang, C., D. R. Simeonov, and D. M. Swank. 2007. The influence of phosphate on the shortening velocity of *Drosophila* jump muscle expressing slow, very fast, and superfast myosin isoforms. *Biophys. J.* 92:299a.
46. Fischer, S., B. Windshugel, D. Horak, K. C. Holmes, and J. C. Smith. 2005. Structural mechanism of the recovery stroke in the myosin molecular motor. *Proc. Natl. Acad. Sci. USA.* 102:6873–6878.
47. Tsiavaliaris, G., S. Fujita-Becker, R. Batra, D. I. Levitsky, F. J. Kull, M. A. Geeves, and D. J. Manstein. 2002. Mutations in the relay loop region result in dominant-negative inhibition of myosin II function in *Dictyostelium*. *EMBO Rep.* 3:1099–1105.
48. Shih, W. M., and J. A. Spudich. 2001. The myosin relay helix to converter interface remains intact throughout the actomyosin ATPase cycle. *J. Biol. Chem.* 276:19491–19494.
49. Sasaki, N., R. Ohkura, and K. Sutoh. 2003. *Dictyostelium* myosin II mutations that uncouple the converter swing and ATP hydrolysis cycle. *Biochemistry.* 42:90–95.
50. Littlefield, K. P., D. M. Swank, B. M. Sanchez, A. F. Knowles, D. M. Warshaw, and S. I. Bernstein. 2003. The converter domain modulates kinetic properties of *Drosophila* myosin. *Am. J. Physiol.* 284:C1031–C1038.
51. Swank, D. M., A. F. Knowles, W. A. Kronert, J. A. Suggs, G. E. Morrill, M. Nikkhoy, G. G. Manipon, and S. I. Bernstein. 2003. Variable N-terminal regions of muscle myosin heavy chain modulate ATPase rate and actin sliding velocity. *J. Biol. Chem.* 278:17475–17482.